A microfabricated microconcentrator for sensors and gas chromatography

Minhee Kim, Somenath Mitra*

Department of Chemistry and Environmental Science, New Jersey Institute of Technology, University Heights, Newark, NJ 07102-1982, USA

Abstract

The key component in trace analysis is the concentration step where the analytes are accumulated before the analysis. This paper presents the development of a micromachined microconcentrator that can be used to enhance the sensitivity of microsensors. Another application demonstrated here is a concentrator-injector for a gas chromatograph. The microconcentrators were fabricated on a 6-in. silicon substrate using standard photolithographic techniques (1 in.=2.54 cm). The channels were lined with a resistive layer, through which an electric current could be passed to cause ohmic heating. The preconcentration was done on a thin-film polymeric layer deposited above the heater in the channel. Rapid heating of the resistive layer caused the ''desorption pulse'' to be injected into the sensor, or onto a GC column. Due to their small size, the microconcentrators could be fabricated 20 to 50 (depending upon the size) at a time on a 6-in. silicon wafer. This paper presents the development and characterization of the microconcentrator. It was found that the microconcentrator performed well as a concentrator, and as an injector for GC. A 14-fold enrichment factor was achieved. The microconcentrator exhibited long-term stability in response, with typical relative standard deviation of between 3 and 5%.
© 2003 Elsevier Science B.V. All rights reserved.

Keywords: Chip technology; Microconcentrator; Instrumentation; Sample handling

1. Introduction

Environmental monitoring requires the measurement of pollutants at trace concentrations (ppm to ppt), because even at these levels they pose a threat to human health and to the environment. A variety of conventional laboratory-based analytical techniques are used for pollution monitoring. Currently, gas chromatography, mass spectrometry and Fourier transform infrared spectrometry (FTIR) are the most commonly used instruments [1–7]. These techniques have excellent merits in terms of sensitivity, detection limit and other performance characteristics [7–10]. However, they are relatively large, expensive and do not lend themselves to easy portability.

The increasing needs for inexpensive, small monitoring devices have added new impetus to miniaturize analysis systems. It is well-known that miniaturization offers functional and economic benefits such as a reduction in sample size, decrease in reagent consumption and inexpensive mass production [11]. Advancements in thin-film technologies have ex-

panded the range of possible microsensor designs. On the other hand, micromachining processes, particularly anisotropic and plasma etching, and the sacrificial layer method make possible the construction of a variety of three-dimensional structures. It is feasible to employ these methods to produce sophisticated, low power integrated sensing systems at a modest cost [12,13]. The high degree of reproducibility and the relatively small size of these devices enhance both performance and the potential for practical applications.

Development of several microsensors has been reported [13,14]. Tin-oxide based sensors have been widely used in gas sensing [14–16]. An important environmental application is the detection of low concentration toxic gases (i.e. CO, NO_2, O_3, etc.). SnO_2 films are commonly used as gas sensors due to their high sensitivity to different gases, low production cost, and the ease of use. Surface acoustic wave (SAW) sensors are another widely used class of highly sensitive environmental sensors [17,18]. A coated SAW device acts as a chemical sensor by adsorbing analytes on its surface. A mass loading on the surface results in a change in propagation velocity and a corresponding phase shift. Schottky-diode-type sensors have also been used in gas sensing [19]. When an analyte diffuses towards the interface between the metal and the insulting layers of a diode, the height of the Schottky barrier diminishes, leading to a change in either the forward voltage or the reverse current. Many chemical species can be detected using electrochemical sensors. An example of a solid electrolyte electrochemical sensor is the ZrO_2-based high-temperature oxygen sensor [20]. This sensor is operated at 650 °C to ensure the ionic conductivity of ZrO_2.

Micromachined gas chromatographs have also been developed [21,22]. GC columns have been etched on silicon, and diaphragm-based valves have been developed as GC injectors [23]. Micromachined thermal conductivity detectors have been successfully made, and are commercially available. A completely micromachined GC could potentially serve as a microsensor.

In principle, sensors and other microdevices can provide real-time (or near real-time), on-line measurements. It is desirable that they be completely automated, and not require additional chemical re-

agents or sample preconditioning. However, the absence of memory effects, high sensitivity, selectivity, reproducibility, short response time and long-term stability are prerequisites for their real-world applicability [18]. The limited success of microsensors is due to the inability to meet some of these requirements. In trace analysis, such as in environmental monitoring, the biggest drawback has been the low sensitivity, and the high detection limits of the sensors [24].

One way to enhance sensitivity in any measurement is to provide some kind of preconcentration. Sorbent trapping in air sampling, solid-phase extraction and SPME are common examples of preconcentration [25,26]. This allows a larger amount of analyte to be concentrated and then released into a detection device. Larger sample throughput in terms of the mass of analyte per unit time results in a higher signal-to-noise ratio.

Over the last few years, we have reported the use of a microtrap as a concentration plus injection device for continuous monitoring of organics in gas streams by gas chromatography, mass spectrometry, or by a non-methane organic carbon (NMOC) analyzer [27–30]. The microtrap is a small sorbent trap. Sample passes continuously through it, and periodic electrical heating releases the adsorbed analytes as a ''concentration pulse'', which serves as an injection for the detection system. Its small size allows it to be cycled at high frequency, and the preconcentration effect allows ppb level detection.

It is envisioned that the sensitivity of a microsensor (or any other microdevice) can be enhanced by providing on-line preconcentration. The objective of this research is to micromachine a concentrator (referred to as the microconcentrator) on a silicon substrate, that can be integrated with a sensor, or a micromachined GC to enhance the signal-to-noise ratio. Basically, the microconcentrator is a miniaturized sorbent trap fabricated on a microchip. It is to be made on a silicon substrate so that a sensor can be integrated on the same chip. The microconcentrator is put on-line with the sample stream, and is operated at a fixed frequency. In principle, it is similar to the microtrap for GC and MS described above [27–30]. It is composed of microchannels etched in silicon. The channels are lined with a microheater for in-situ heating. The preconcentration is done on a thin-film

polymeric layer deposited above the heater in the channel. Rapid heating by the channel heater generates a ''desorption pulse'' to be injected into a detector, or, a sensor. This paper presents the development and characterization of the microconcentrator.

2. Experimental

The microconcentrators were fabricated on $\langle 100 \rangle$ oriented, 6-in., p-type, single side polished silicon wafers, with a thickness of 575 μm and a resistivity of 10–25 Ω cm (1 in.=2.54 cm). The chip layout was done on a Sun Sparc workstation using the IC tool in Mentor Graphics (Wilsonville, OR, USA). All fabrications were done at the New Jersey Institute of Technology Microelectronics Research Center class 10 cleanroom. Fig. 1 shows the step-by-step processing of the wafer and its cross sectional view after each step.

The first step was steam oxidation of the wafers to grow the oxide layer. This was followed by low-pressure chemical vapor deposition (LPCVD) of the nitride layer. Then the wafers with 2000 Å thick oxide with standard deviation of ± 32 Å and 1550 Å thick nitride with standard deviation of ± 18 Å were patterned using standard UV lithography. The patterned wafers were etched using reactive ion etching (RIE). The RIE is a combination of plasma etching and ion beam removal of the surface layer. It has the major advantage of etching the silicon dioxide over the silicon layers. After this, anisotropic etching with KOH was performed at 95 °C at an etch rate of 1.66 mm/min. Etching the $\langle 100 \rangle$ oriented silicon wafers in KOH (45%, w/v) produced wells with 54° angle sidewalls (based on scanning electron microscopy (SEM) image). Since the substrate was $\langle 100 \rangle$ oriented, the chemical wet etching produced channels anisotropically with low aspect ratios. As a result, the channel geometry was trapezoidal. Several channel configurations were fabricated with widths between 50 and 456 μm, depths between 35 and 350 μm and lengths between 6 and 19 cm. The separation distance between the channels was varied such that the entire structure was less than 1 cm^2 in area.

A thin-film of metal deposited in the channel

served as the heating element. The metal deposition was carried out by sputtering. The metal source used in this study was an aluminum alloy, which was 99% aluminum, the rest being silicon (0.5 to 0.8%) and copper (0.1 to 0.5%). The main reason for using the silicon–aluminum alloy was to prevent the silicon in the wafer from reacting with the deposited aluminum, which could cause spiking, or shorted circuits.

Then the heater was coated with Spin-On-Glass (SOG, Honeywell, CA, USA) because the organic polymers to be used as the absorbing film have low adhesivity to silicon and metal. Glass surfaces also provide the potential of different chemical modifications using organosilanes. The glass coat was applied by spinning SOG over the surface of the wafer. The thickness was controlled by the speed of the spinner. Four milliliters of SOG were applied on a 6-in. wafer and spun at 2000 rev./min for 2.0 s to achieve an ~1 μm film. This was followed by hard plate baking at 80, 150 and 250 °C for 40 s each. Then the wafers were placed in the furnace for curing at 425 °C for 60 min.

Thin films of commercially available gas chromatography stationary phase, OV17 (50% polymethyl–50% phenyl-phase, from Supelco, Supelco Park, PA, USA) were deposited on the microconcentrator by spin coating (2000 rev./min for 20 s). This formed the absorbing layer. The thickness of the polymeric layer was varied by adjusting spin-coating conditions. Then the wafers were placed in the oven for baking at 120 °C for 48 h.

Bonding of patterned silicon to quartz glass was carried out using WaferGrip (Dynatex, Santa Rosa, CA, USA). WaferGrip is an advanced composite film adhesive engineered to bond wafers and other substrates during dicing, grinding, lapping and polishing. WaferGrip is heat activated and was rated by the manufacturer to have uniform thickness. The adhesive layer of WaferGrip was compressed on the substrate under vacuum using a wafer bonder. This resulted in a leak-proof device. The cross section view of the microconcentrator is presented in Fig. 2A. Fig. 2B shows the photograph of the microconcentrator, and it is compared to a US penny.

The microconcentrator is a general-purpose device that can be used with any sensor or detector. Here it was tested with a conventional flame ionization

1500Å Si_3N_4

2000Å SiO_2

Photolithography of Si_3N_4 and SiO_2

KOH etching

Deposition of Aluminum alloys

Spin-on-glass coating
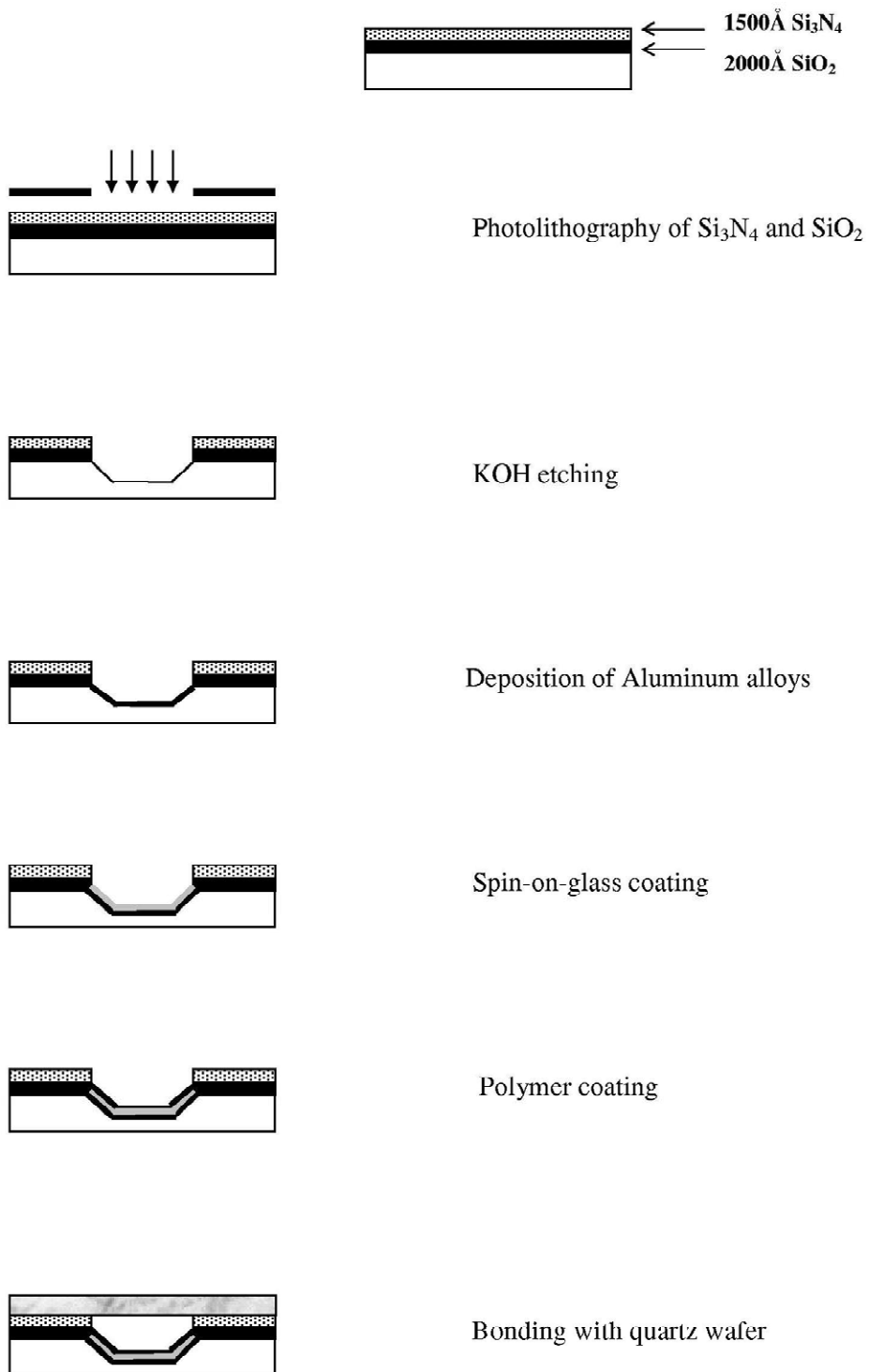
Polymer coating

Bonding with quartz wafer

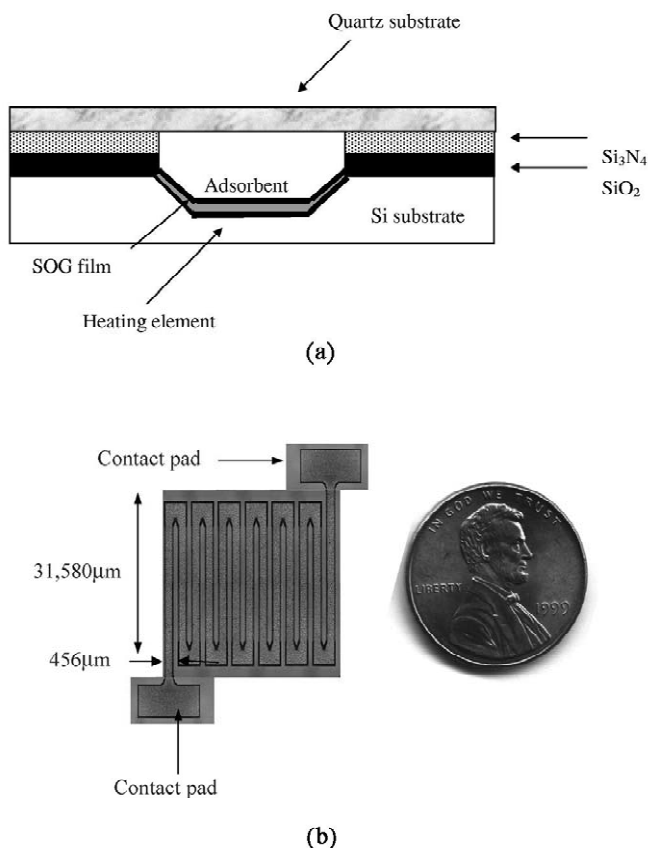Fig. 1. Steps in the fabrication of the microconcentrator.

Fig. 2. (A) Cross section of the etched channel of the microfabricated microconcentrator. (B) Photograph of the microconcentrator. It is compared to a US penny.

detection (FID) system. The experimental system used in this study is shown in Fig. 3. In some experiments, the microconcentrator was cooled by placing over an ice pack. An SRI Instrument Model 8600/9300 portable GC system equipped with an FID system was used for analysis. In some tests, a 30 m×0.53 mm I.D. capillary column (DB-624, J&W Scientific) was used, and repeat injections were made under isothermal conditions to generate a series of chromatograms. Standard gases such as air, nitrogen, and hydrogen were purchased from Matheson Gas (NJ, USA). Nitrogen was used as the carrier gas, and the flow-rate was 7 ml/min. Data acquisition was carried out using the Peaksimple Data System supplied by SRI Instruments. Calibration, qualitative/quantitative analysis, documentation of

analytical results, and report output were handled by this system.

The standard gaseous stream was generated using the diffusion tube method [31], and typical concentrations were between 5 and 20 ppmv. Steady streams of benzene, toluene or ethyl benzene were generated by diffusing a controlled amount of the analyte from the diffusion capillary into a flow of N_2. The organic vapors were adsorbed by the microconcentrator. The preconcentration was done on the thin-film polymeric layer deposited in the channel. A pulse of electric current (a.c.) was applied to the microconcentrator at predetermined intervals to desorb the trapped organics. The duration of the pulse was between 1 and 3 s. Rapid heating of the conductive layer caused the ''desorption pulse'' to be
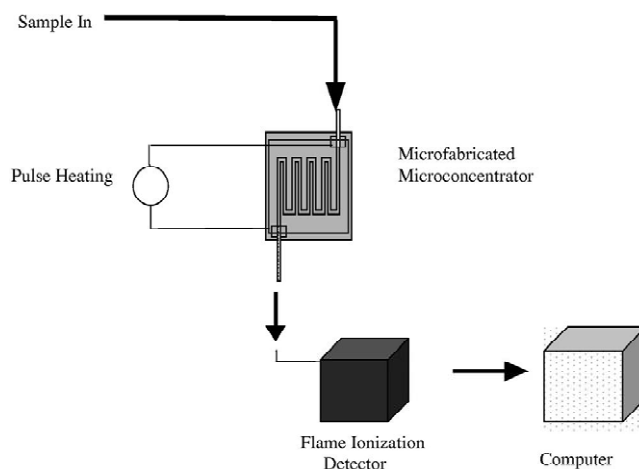
Fig. 3. Schematic diagram of the experimental system.

injected into the detector. A microprocessor-based controller was used to control the interval, and the duration of the electrical pulses to the heater. More details on the pulse heating have been presented elsewhere [27–30].

3. Results and discussion

3.1. Heating characteristics of the microchannel heater

The key component in the microconcentrator is the heating element embedded in the channel. The heating characteristics of the channel heater were studied. The temperature of the microchannel was measured using a 50-μm thermocouple. A typical temperature profile as a function of time is plotted in Fig. 4. The temperature depended upon several factors such as heater design, applied voltage etc. [32]. For the heater presented here, temperature as high as 200 °C could be reached in less than 10 s. The SOG provided a resistance to heat transfer and the maximum temperature reduced to 120 °C. It should be noted that the thermocouple had a slow response, and the real heat-up rate could be somewhat higher. Detailed heating characteristics of such thin-film heaters have been presented elsewhere, and the heater stability during multiple cycling has been

demonstrated [32]. The heated channel in this study had a width of 450 μm, depth of 300 μm, and the total length was 16 cm.

3.2. On-line microconcentrator

The microconcentrator was put on-line with the sample stream. The gaseous sample containing the analyte was introduced into the detector through the microconcentrator. The analytes were trapped in the polymer film and could be thermally desorbed by electrical heating. The desorption was achieved by resistive heating by a current pulse (1 to 3 s). Rapid desorption was essential for producing a sharp concentration pulse to provide high throughput in terms of mass of sample per second. The mode of operation for continuous monitoring was that electrical pulses (injections) were made at fixed intervals of time, and corresponding to each injection, a signal pulse was obtained. Continuous monitoring using the microconcentrator was demonstrated by monitoring a stream of organic vapors. As seen in Fig. 5, the microconcentrator generated a series of signal pulses corresponding to a sequence of injections. The peaks here represent a signal enhancement by a factor of 14, i.e. the signal from the microconcentrator was 14 times that obtained by direct sample introduction. Reproducibility in terms of peak height was excellent, and injection pulses could be continued indefi-
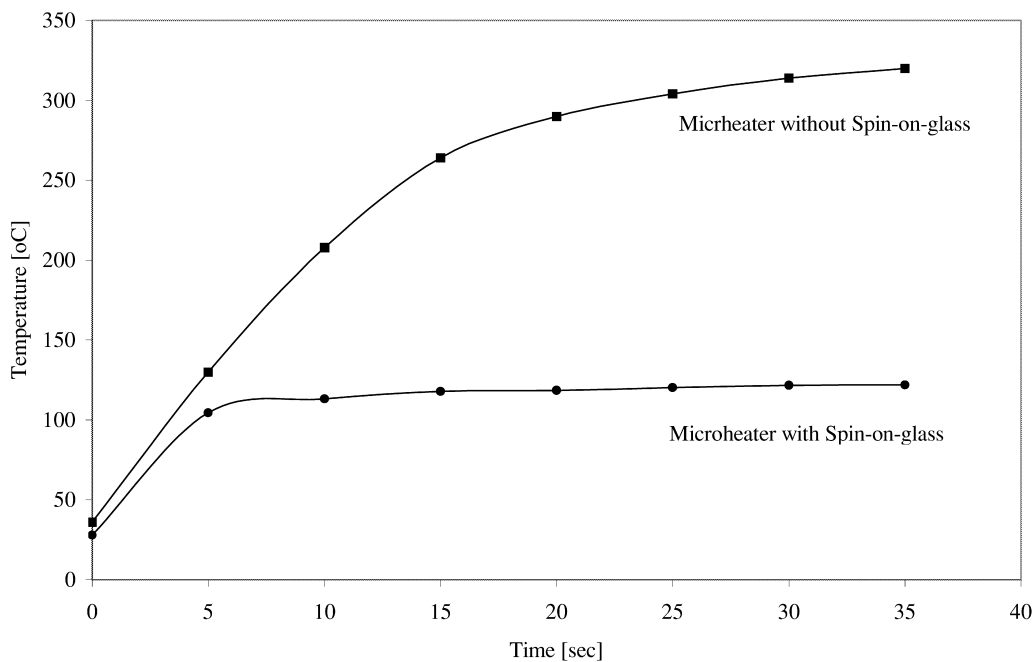
Fig. 4. Temperature characteristics of the heater embedded in the microconcentrator.

nitely. The relative standard deviation in peak height based on six repeat injections was 1.02%.

Both adsorption and desorption processes played important roles in the on-line microconcentrator operation. In a previous study, the effect of capacity factor in a conventional packed tube microtrap was
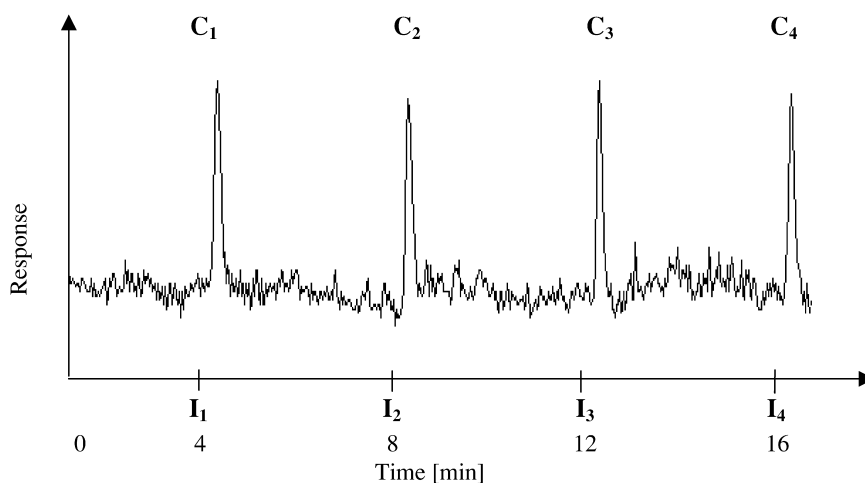

Fig. 5. Continuous monitoring of a stream containing organics using the microconcentrator shown in Fig. 2B. Corresponding to each injection I_1, I_2, I_3 ... a response C_1, C_2, C_3 ... was obtained.

described [33]. Similar ideas are applicable here. The adsorption capacity in terms of analyte breakthrough, and the desorption efficiency are important parameters. Because of its small dimensions, only a small mass of the sorbing phase could be coated inside. Consequently, the microconcentrator had inherently low capacity and was prone to breakthrough.

The breakthrough characteristics could be studied from the peak shape. The sample flowed continuously through the microconcentrator. When the microconcentrator was heated, a desorption peak was observed. The analytes were re-adsorbed in the microconcentrator as it cooled. This lowered the baseline into the negative territory appearing as a negative peak. As the sample began to breakthrough, the detector response increased back to the baseline. The width of the negative peak has been shown to equal the breakthrough time, t_b, measured by frontal chromatography [28]. The desorption generated a positive concentration profile while the immediate sample readsorption generated a negative one. Thus, a microconcentrator peak contained a positive and a negative part as shown in Fig. 6. The time interval AD in Fig. 6 is the time taken by the sample to migrate through the microconcentrator. This is denoted as:

$$t_b = (k + 1)L/u \tag{1}$$

where L is the length of the microconcentrator, u is the linear velocity of the sample and k is the capacity factor of the sample in the microconcentrator stationary phase [33]. The capacity factor could be increased by using a stronger sorbing phase, or by operating at a lower temperature. As the capacity factor increased, t_b increased, and the negative peak became shallow and appeared to merge with the baseline. So, the remaining positive peak resembled a conventional concentration spike without a negative profile [33]. Fig. 6 represents a low-capacity microtrap with a relatively thin-film coating (0.7 µm) where the negative peak is pronounced, whereas Fig. 5 shows the response of a higher-capacity microconcentrator with a thicker polymer film (2.4 µm) and without the negative profile. A microconcen-
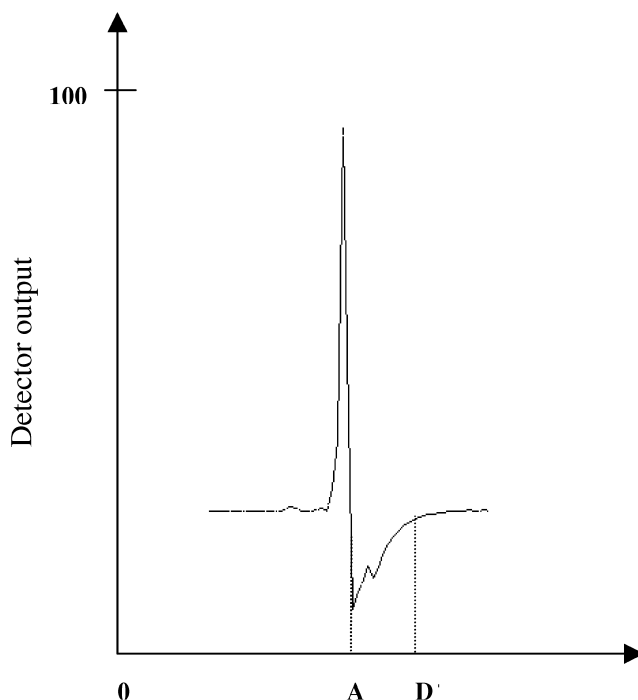

Fig. 6. Characteristic peak from a low capacity microconcentrator which shows a pronounced negative peak.

trator with a higher capacity factor allowed longer breakthrough time, and generated peaks without the negative parts.

The microconcentrator response as a function of injection interval was studied. As the interval increased, the amount of sample trapped in the microconcentrator increased. However, once the interval equaled t_b, the sample began to breakthrough, and the response could not be increased further. This is shown in Fig. 7. The response profile showed a linear increase in response up to t_b, followed by a constant response beyond t_b. It was seen that the temperature affected microconcentrator operations; lower temperature increases t_b.

Linearity in microconcentrator response was observed as a function of concentration. The concentration range studied here was from 20 to 800 ppm of toluene. Since the amount of sample trapped in the microconcentrator was proportional to the concentration of the stream flowing in, its response was proportional to sample concentration. At a longer injection interval, the larger amount of trapped sample resulted in a higher response. The microconcentrator could be operated at any injection interval, either longer or shorter than t_b. Once beyond t_b, the sensitivity of the calibration curve did not increase with injection interval. Operating it at higher frequency resulted in faster monitoring, but allowed less time for sample accumulation, thus, lower sensitivity.

3.3. Microconcentrator as a GC injector

The microconcentrator was also used as a GC injector. A mixture of benzene, toluene and xylene was used as the sample stream. A short megabore column was used for the separation of these compounds. A series of injections were made, and a chromatogram was obtained corresponding to each injection. As shown in Fig. 8, sharp peaks comparable to a conventional injection port were observed. This demonstrated that the injection band was narrow due to the rapid desorption from the microconcentrator. Reproducibility of retention time and peak height were very good. The relative standard deviation in peak height was consistently between 2 and 5%. The detection limit here is dependent on the detector and could be lowered using a more sensitive laboratory instrument. The microconcentrator was found to be rugged and could be operated practically indefinitely. Experience in our laboratory showed no deterioration in performance over a year of operation.
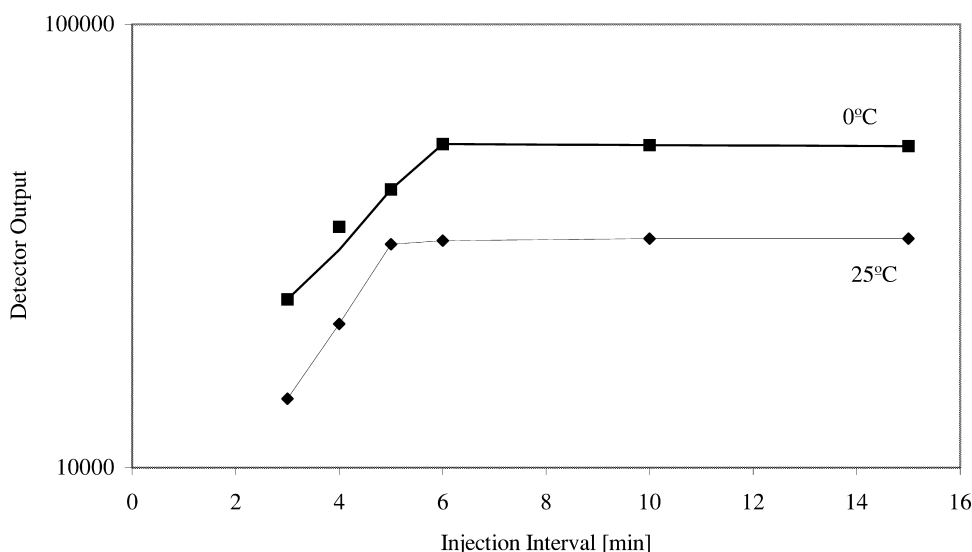

Fig. 7. Microconcentrator response as a function of injection interval at 0 °C and 25 °C. Toluene was used as the analyte.
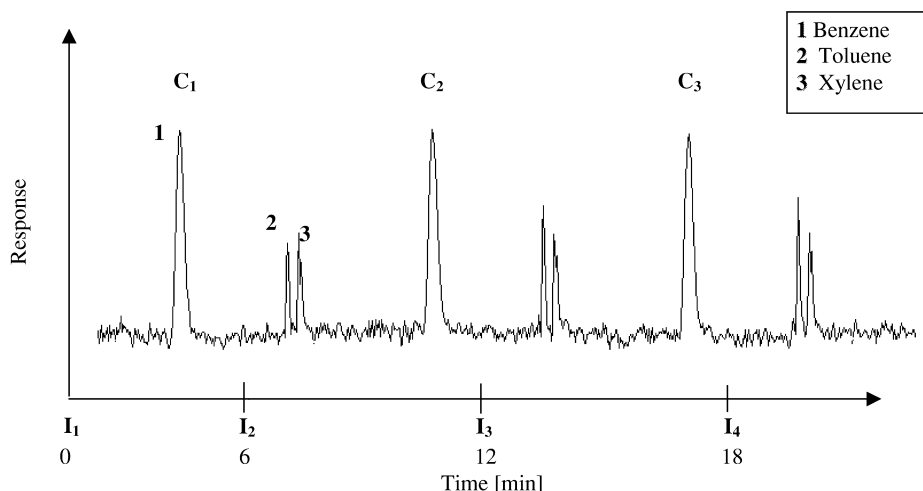
Fig. 8. Continuous monitoring of a stream containing ppm levels of benzene, toluene and xylene using the microconcentrator shown in Fig. 2B. Corresponding to each injection I_1, I_2, I_3 . . . a chromatogram C_1, C_2, C_3 . . . was obtained.

4. Conclusions

The fabrication and characterization of a microfabricated microconcentrator has been presented. The preconcentration effect enhanced sensitivity, and it was possible to use it as an injector for GC. The microconcentrator response was stable, and it exhibited good precision.

References

[1] J.J. Johnston, D.A. Goldade, D.J. Kohler, J.L. Cummings, Environ. Sci. Technol. 34 (2000) 1856.
[2] K. Dobosiewicz, K. Luks-Betlej, D. Bodzek, Water Air Soil Pollut. 118 (2000) 101.
[3] R.T. Short, D.P. Fries, G.P.G. Kibelka, S.K. Toler, P.G. Wenner, R.H. Byrne, in: Oceans Conference Recored (IEEE), Honolulu, HI, Vol. 1, 2001, p. 256.
[4] J.A. De Gouw, C.J. Howard, T.G. Custer, B.M. Baker, R. Fall, Environ. Sci. Technol. 34 (2000) 2640.
[5] L. Charles, L.S. Riter, R.G. Riter, Anal. Chem. 73 (2001) 5061.
[6] B. Galle, J. Samuelsson, B.H. Svensson, G. Borjesson, Environ. Sci. Technol. 35 (2001) 21.
[7] X. Hu, J. Nicholas, J.J. Zhang, M. Temi, P. De Filippis, P.K. Pradeep, Fuel 81 (2002) 1259.
[8] Y. Takao, Y. Kanda, Rev. Sci. Instrum. 67 (1996) 198.
[9] S. Shelley, Chem. Eng. (1991) 30.
[10] Q.H. Wu, K.M. Lee, C.C. Liu, Sensors Actuators B 13 (1993) 13.
[11] B. van der Schoot, E. Verpoorte, S. Jeanneret, A. Manz, N. de Rooij, in: Proceedings 1st International Symposium on Micro Total Analysis Systems, Twente, The Netherlands, 1994, p. 21.
[12] S. Zimmermann, S. Wischhusen, J. Mueller, Sensors Actuators B 63 (3) (2000) 159.
[13] H. Suzuki, Mater. Sci. Eng. C: Biomimet. Supramol. Syst. 12 (2000) 55.
[14] Th. Becker, St. Muehlberger, Chr. Bosch-v. Braunmuehl, G. Mueller, Th. Ziemann, K.V. Hechtenberg, Sensors Actuators B 69 (2000) 108.
[15] C. Bulpitt, S.C. Tsang, Sensors Actuators B 69 (2000) 100.
[16] A.C. Romain, J. Nicolas, V. Wiertz, J. Maternova, Ph. Andre, Sensors Actuators B 62 (2000) 73.
[17] M. Fang, K. Vetelino, M. Rothery, J. Hines, G.C. Frye, Sensors Actuators B 56 (1999) 155.
[18] J. Reibel, U. Stahla, T. Wessa, M. Rapp, Sensors Actuators B 65 (2000) 173.
[19] C.K. Kim, J.H. Lee, Y.H. Lee, N.I. Cho, D.J. Kim, Sensors Actuators B 66 (1) (2000) 116.

[20] J. Deng, W. Zhu, O.K. Tan, X. Yao, Sensors Actuators B 77 (1–2) (2001) 416.

[21] Y. Kawamura, S. Konishi, N. Masataka, Fusion Eng. Design 58–59 (2001) 389.

[22] Agilent 3000 Micro GC, Agilent Technologies, USA, 2002.

[23] H. Noh, P.J. Hesketh, G.C. Frye-Mason, in: Proceedings of the IEEE Micro Electro Mechanical Systems (MEMS), Las Vegas, NV, 2002, p. 20.

[24] W. Gopel, Sensors Actuators A 56 (1996) 83.

[25] M.J. Gardner, H.R. Rogers, S.D.W. Comber, J. Water Supply 49 (2000) 103.

[26] J. Beltran, F.J. Lopez, O. Cepria, F. Hernandez, J. Chromatogr. A 808 (1998) 257.

[27] Y.H. Xu, S. Mitra, J. Chromatogr. A 688 (1994) 171.

[28] S. Mitra, C. Yun, J. Chromatogr. 648 (1993) 415.

[29] S. Mitra, C. Feng, L. Zhang, W. Ho, G. McAllister, J. Mass Spectrom. 34 (1999) 478.

[30] S. Mitra, Y.H. Xu, W. Chen, G. McAllister, J. Air Waste Manage. Assoc. 48 (1998) 643.

[31] A.C. Savitsky, S. Siggia, Anal. Chem. 44 (1972) 1712.

[32] M. Kim, S. Kishore, D. Misra, S. Mitra, Lab on a Chip, (2003) submitted for publication.

[33] S. Mitra, J.B. Phillips, J. Chromatogr. Sci. 26 (1988) 620.